THE JOURNAL OF PHYSICAL CHEMISTRY A

Article

pubs.acs.org/JPCA

Direct Observation of a Dark State in the Photocycle of a Light-Driven Molecular Motor

Saeed Amirjalayer,*[,†,‡,§] Arjen Cnossen,[∥] Wesley R. Browne,[∥] Ben L. Feringa,[∥] Wybren J. Buma,*[,§] and Sander Woutersen*[,§]

[†]Physikalisches Institut, Westfälische Wilhelms-Universität Münster, Wilhelm-Klemm-Strasse 10, 48149 Münster, Germany

[‡]Center for Nanotechnology, Heisenbergstrasse 11, 48149 Münster, Germany

[§]Molecular Photonics Group, Van 't Hoff Institute for Molecular Science, University of Amsterdam, Science Park 904, 1098XH Amsterdam, The Netherlands

[∥]Stratingh Institute for Chemistry and Zernike Institute for Advanced Materials, University of Groningen, Nijenborgh 4, 9747 AG Groningen, The Netherlands

Supporting Information

ABSTRACT: Controlling the excited-state properties of light driven molecular machines is crucial to achieving high efficiency and directed functionality. A key challenge in achieving control lies in unravelling the complex photodynamics and especially in identifying the role played by dark states. Here we use the structure sensitivity and high time resolution of UV-pump/IR-probe spectroscopy to build a detailed and comprehensive model of the structural evolution of light driven molecular rotors. The photodynamics of these chiral overcrowded alkene derivatives are determined by two close-lying excited electronic states. The potential energy landscape of these "bright" and "dark" states gives rise to a broad excited-state electronic absorption band over the entire mid-IR range that is probed for the first time and modeled by quantum mechanical calculations. The transient IR vibrational fingerprints observed in our studies allow for an unambiguous identification of the identity of the "dark" electronic excited state from which the photon's energy is converted into motion, and thereby pave the way for tuning the quantum yield of future molecular rotors based on this structural motif.

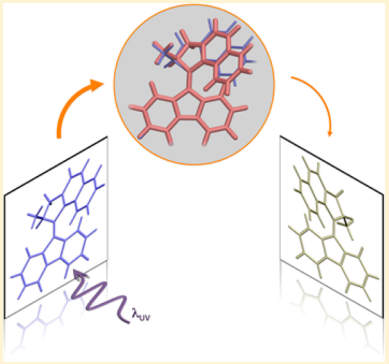

INTRODUCTION

One of the key challenges in the development of novel materials is the ability to tune and control their macroscopic physical and chemical properties on a molecular level by external stimuli.[1−5] Such a degree of control is challenging but crucial for a wide range of applications ranging from catalysis to pharmacological and medical applications.[6−11] In photoactive materials light absorbed by chromophores can be converted into directed functionality, typically by means of photoinduced isomerization of nitrogen or carbon containing double bonds and pericyclic reactions.[12−27] Indeed, *E*−*Z* isomerization results in large amplitude changes in structure as well as chemical and physical properties.[28−32]

Molecular motors based on overcrowded alkenes are particularly attractive due to the synthetically tunable properties, such as thermal stability, absorption spectra, etc., and therefore are readily applied to a wide range of functional systems. However, although the thermally activated step in the unidirectional rotary cycle is well understood and is now largely predictable, the photochemical properties and especially photochemical quantum yields are less well understood. Hence both from a fundamental perspective and in achieving the goal of complete molecular design, gaining insight into the excited-state properties of light driven molecular-sized machines is essential.[33]

The overcrowded alkene-based molecular rotary motors are composed of a central carbon−carbon double bond (the axle) embedded in an intrinsically chiral environment. The unidirectional rotational cycle starts with a photoinduced *E*−*Z* isomerization around the central C═C bond, generating a metastable isomer P* (Figure 1), which relaxes thermally to the stable isomer P, which in the case of a symmetric stator unit is identical to I. This isomer marks half of the rotation cycle and is the starting point for a second photoinduced isomerization step that leads again to a metastable isomer. Thermally activated conformational isomerization of this isomer brings the system back to its initial state. Overall, the rotor part has then performed a complete rotation with respect to the stator unit of the molecular motor.

Although the rotation includes both photochemical and thermal steps that involve different parts of the motor, the structural evolution is largely governed by the excited-state properties of the central C═C group, which, in turn, are

Received: September 23, 2016
Revised: September 28, 2016
Published: September 29, 2016

DOI: 10.1021/acs.jpca.6b09644
J. Phys. Chem. A 2016, 120, 8606−8612

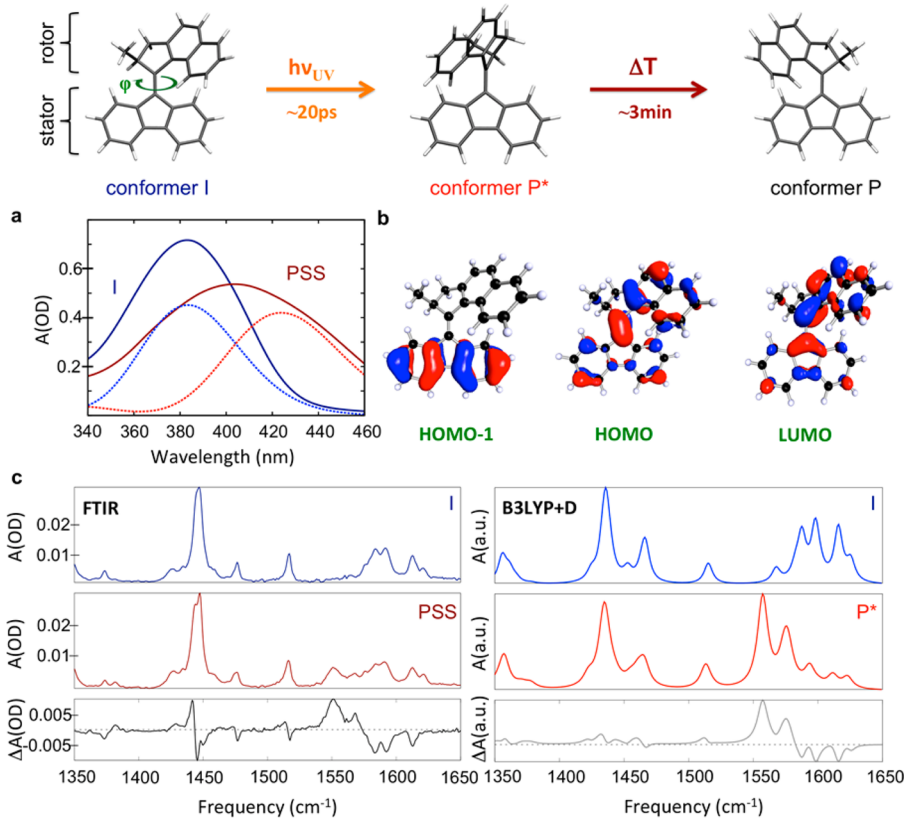

Figure 1. Unidirectional motion of the unidirectional motor starting from the thermally stable conformer (I) via the product of the photoinitiated step (P*) to the thermally stable conformer (P) (optimized geometries on the B3LYP+D/aug-cc-pVDZ level): (a) experimental and calculated (light color and dotted line) UV−vis spectra of conformer I and P*; (b) molecular orbitals of the initial conformer; (c) experimental and calculated IR spectra (B3LYP+D/aug-cc-pVDZ) of the initial state (blue) and final state (red). In both the measured UV/vis absorption and FTIR spectra at the photostationary state (PSS), I and P* are present in a 25:75 ratio.[60]

dictated by the potential energy surfaces of the excited states that are accessed upon electronic excitation. Despite the large number of theoretical[34−41] and experimental studies[42−44] that have focused on characterizing this process, there are several key questions outstanding including identification of the main structural coordinates and the role of various electronic states involved in the excited-state dynamics. Time-resolved studies are essential to elucidate these dynamics but have thus far focused on probing the change in the electronic structure after photoexcitation through UV/vis absorption[42,43] and fluorescence[43,44] studies. These techniques offer a high time resolution but provide only indirect information as to how the structure evolves spatially over time. In the present contribution we show that this information can be obtained through a combination of picosecond time-resolved vibrational spectroscopy of the electronically excited states together with quantum-mechanical calculations.

METHODS

The setup for the time-resolved infrared measurements has been described in detail previously.[45] Mid-IR probe pulses were generated using an amplified Ti:sapphire system (Spectra-Physics Hurricane, 600 μJ, repetition rate 1 kHz) pumping a commercial BBO-based OPA (Spectra-Physics OPA-800C), the signal and idler output of which were difference-frequency-mixed in $AgGaS_2$. UV pump pulses (400 nm, ∼1 μJ) were generated by doubling part of the output of the Ti:sapphire laser. The diameter of the UV pump focus was ∼180−200 μm; that of the IR probe focus, ∼150 μm. The sample cell with CaF_2 windows spaced by 500 μm was placed in the IR focus. To avoid accumulation of the thermally unstable conformer P* during the measurements, a flow cell was used. With a Newport ESP300 translation stage, the pump−probe delay time was scanned by mechanically adjusting the beam path of the UV pump. The temporal resolution of 200 fs has been determined from the full width at half-maximum of the pump probe cross-correlation function. The pump pulse was chopped at 500 Hz, and transient spectra were obtained by subtracting nonpumped absorption spectra from the pumped absorption spectra, both of which were recorded by spectrally dispersing the probe pulses using an Oriel MS260i spectrograph and measuring the frequency-dependent IR intensity using a 2 × 32 HgCdTe detector array (Infrared Associates). Compound I was available from earlier studies (see ref 44). In all experiments we investigate a 10mM solution of compound I in deuterated cyclohexane (Aldrich, 99.6 atom% D).

For the investigation of the ground-state conformers (including vertical excitation energies and forces acting at the Franck−Condon point) quantum mechanical calculations were performed using the TURBOMOLE suite of programs.[46] Geometry optimization and normal-mode analysis were performed by (time-dependent) density functional theory ((TD)-DFT) using the hybrid functional B3LYP.[47] For the geometry optimization the D3 correction method of Grimme et al.[48] was used to include dispersion effects. For all elements the cc-pVDZ or aug-cc-pVDZ basis sets were employed, respectively.[49,50] Second derivatives were computed analytically

DOI: 10.1021/acs.jpca.6b09644
J. Phys. Chem. A 2016, 120, 8606−8612

with the AOFORCE module. The vibrational frequencies have been scaled by 0.98. Post-Hartree−Fock calculations were performed on the basis of spin-component scaled second-order Møller−Plesset perturbation theory[51] and the approximate coupled-cluster singles-and-doubles model CC2. All perturbation method calculations were performed using the resolution of identity (RI) approximation[52] and the efficient RICC2 module[53] implemented in the TURBOMOLE package together with the standard auxiliary basis sets.[50] The Gaussian09 program package[54] was employed to study the excited-state properties in more detail and in particular to optimize the structure of the dark-state species. Geometry optimization and normal-mode analysis were performed in the framework of TD-DFT at the B3LYP/cc-pVDZ level.[49,55−59]

RESULT AND DISCUSSION

The structural evolution from the initial state I to isomer P* (Figure 1) was considered first in terms of the spectral properties of the initial state and the first metastable product (P*). The steady-state UV/vis absorption spectra of the two isomers are distinct, reflecting a change in the conjugated π system (Figure 1a). The FTIR spectra of the two isomers (Figure 1c) show that the carbon−carbon stretch and ring vibrations couple to a large degree as a consequence of the extended π system; however, DFT calculations enable us to assign the bands in the 1550−1650 cm^{-1} range as being mainly associated with modes involving the central C═C double bond (Supporting Information). The metastable isomer P* shows a shift of these modes to lower frequencies confirming a decrease in bond strength. Comparison of the optimized geometries of the two isomers (I (P*), CC bond length 1.369 (1.377) Å; CC═CC dihedral angle 14.1° (29.5°)) evidence the corresponding lower π bond character as well.

Time-resolved vibrational spectroscopy[61−67] was employed to achieve the required temporal resolution as well as structural sensitivity to elucidate the structural evolution that follows photoexcitation with a short UV-pump pulse (center wavelength 400 nm). The resulting structural evolution was followed by time-resolved differential absorption spectra in cyclohexane-d_{12} with a time resolution of 200 fs (Figure 2). The transient IR spectra show, as expected, pronounced differences between the IR absorption spectrum of the molecule in the initial and excited states. A first point of note is that the spectrum does not evolve further after ca. 30 ps, and the difference spectrum corresponds perfectly with the difference spectrum obtained upon continuous wave excitation (Figure 1); i.e., the metastable isomer P* has formed fully within the 30 ps after excitation.

The time-resolved IR spectra obtained within the first 30 ps exhibit several remarkable features. The first and most striking is a broad and unstructured absorption over the entire mid-IR range (1200−3000 cm^{-1}). This absorption, which decays rapidly, is particularly prominent at early time delays (<5 ps). Individual absorption bands with remarkably high integrated intensities in the 1400−1600 cm^{-1} range are superimposed on the broad spectral feature. Notably, these bands are significantly broader than the bleached bands in the transient spectra and bands in the FTIR spectra. The solvent response and the dependence of the UV pump intensity (Supporting Information) confirm that these features are intrinsic to the compound and are not due to solvent or two-photon processes.

The width and intensity of the broad excited-state absorption bands excludes that they arise from vibrational transitions. Indeed, the absorbance is closer to that expected for electronic

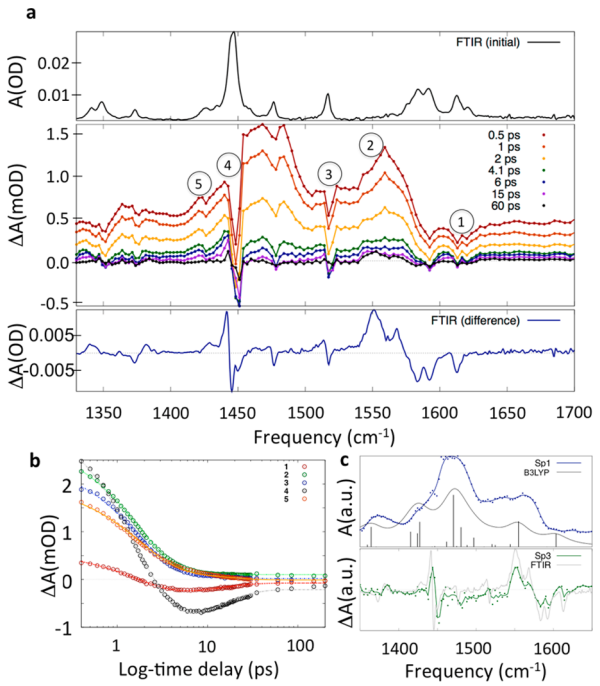

Figure 2. FTIR and time-resolved Infrared spectra of the molecular motor in cyclohexane-d_{12}: (a) FTIR spectra of the thermal stable conformer (initial, solvent corrected, top), UV-ump/IR-probe transient infrared spectra (λ_{UV} = 400 nm) (middle), and difference FTIR spectra between the two ground-state conformers of the molecular motor; (b) kinetics of selected bands and corresponding results of the global fit; (c) species associated spectra (SAS) of species 1 and calculated IR spectra (top) and SAS of the PSS (Sp3) together with FTIR spectra (bottom). Negative bands indicate ground-state bleaching, and positive bands, species created after excitation.

transitions, albeit these typically occur at much higher energies (in the UV/vis range). The electronic excited-state manifold of the compound was therefore investigated computationally. The initial state of the compound (I) shows an absorption band at 390 nm (Figure 1), which is reproduced well by B3LYP/cc-pVDZ calculations in the gas phase (403 nm; f = 0.428). The $S_1 \leftarrow S_0$ transition has predominantly HOMO → LUMO character (Figure 1). In contrast to previous assignments,[42] however, we find that this electronic transition is not localized on the stator but involves to a significant extent excitation from the bonding π orbital of the central double bond to the antibonding π^* orbital (Figure 1). As a consequence, the double bond character of this bond is reduced as well as the barrier to rotation around this bond. In line with calculations on ethylene and its derivatives, we find a dark state (S_2) associated with the HOMO−1 → LUMO excitation at slightly higher excitation energies that is not directly accessible from the ground state (Figure 1, Table 1). Because the HOMO−1 orbital is localized on the aromatic stator unit, S_2 has a significantly larger dipole moment than S_1 (4.3 vs 2.2 D at the SCS-CC2/cc-pVDZ level). It should be emphasized that the description of the lower-lying electronic states in the compound studied here is thus entirely different from ethylene and its derivatives where, as discussed by Salem and others,[68−73] for torsion angles of around 90° the two low-lying electronic states have either a biradical or zwitterionic character depending on the occupation of the two central 2p-orbitals and require multireference methods for a proper description. In the present study, in contrast, we investigate the dynamics occurring at

DOI: 10.1021/acs.jpca.6b09644
J. Phys. Chem. A 2016, 120, 8606−8612

Table 1. Calculated Vertical Excitation Energies (E_{vert}, eV) and Corresponding Oscillator Strength in Brackets of the First Two Excited States of the Molecular Motor at the Optimized S_0 and S_1 Geometries

	B3LYP/aug-cc-pVDZ[a]		SCS-CC2/cc-pVDZ	
geometry	S_0	S_1	S_0	S_1
S_1	3.020 (0.428)	2.228 (0.004)	3.642 (0.583)	2.353 (0.002)
S_2	3.065 (0.963×10^{-3})	2.632 (0.495)	3.662 (0.018)	2.788 (0.592)

[a]For S_0 the optimized structure on the B3LYP+D/aug-cc-pVDZ level was used to calculate the vertical excitation energies.

small torsional angles (*vide infra*) for which the employed single-reference methods not only have been validated.[37] In addition we employ the results of multireference calculations on smaller motor molecules as reported by Liu and Morokuma[34] to make a further comparison with our experimental results.

For vertical excitation our calculations predict that S_1 and S_2 are nearly degenerate (Table 1). They thus strongly suggest that the broad and structureless absorption feature observed in the time-resolved IR spectra is associated with the electronic $S_1 \rightarrow S_2$ transition. The presence of two close-lying states also explains why the induced absorption bands have such high intensities. Our calculations show that the energy gap between the two states strongly depends on structural parameters such as the C=C bond length that are involved in the 1400−1600 cm^{-1} normal modes. For these modes one therefore expects that their transition moments will be enhanced by vibronic coupling as is indeed observed. The conclusion that the excited-state dynamics of the molecular rotor should be described in a multistate model is further supported by recent multireference calculations on smaller rotor molecules that also find very small energy differences between the S_1 and S_2 states.[34]

The excited-state dynamics were elucidated further using a global analysis of the transient spectra, which shows that the spectra can be described well with two exponential decay terms with time constants of 1.53 ± 0.03 and 12 ± 1 ps. We note that our experiments have a time resolution of 150−200 fs and therefore do not allow observation and confirmation of the ultrafast dynamics reported previously in fluorescence-upconversion studies.[42] Species-associated spectra (SAS) (Supplementary Figure 2) were derived by using a two-step sequential kinetic model.

The SAS of the first species shows an overall background signal with broad and intense features superimposed on it that indicate vibronic coupling. Furthermore, the increase (decrease) of absorbance in the 1550 (1600) cm^{-1} region indicates a substantial change in bond character of the central double bond (Figure 2c). This spectrum was related to the structure of this excited-state species using excited-state geometry optimizations. Full optimization of the "dark" state without any structural constrains associated with the HOMO−1 → LUMO excitation leads to a stable minimum that can be reached from the Franck−Condon excited geometry by relatively small structural changes (Supplementary Figure 4), and an excited-state IR absorption spectrum that is in good agreement with the SAS of species 1 (Figure 2). It is notable that for a proper comparison with the experimental spectrum, the theoretically predicted stick spectrum needs to be convolved with 20 cm^{-1} Gaussian line shapes, suggesting that in the "dark" state a wide range of structures is sampled. Our experiments and calculations thus demonstrate that excitation and excited-state decay involve two different electronic states. In earlier studies, time-resolved fluorescence and visible absorption data[42−44] were interpreted in terms of a decay from a single, isolated electronic state decaying to the ground state after structural relaxation in the excited state. The present data show that the S_1 state actually decays to an intermediate, dark electronic state, and from there to the ground state.

In the SAS of the second species (Supplementary Figure 2) the broad background is absent, and bands have widths comparable to those in the S_0 state. The absence of the broad background indicates that this species is no longer in an electronically excited state but back in the (vibrationally hot) electronic ground state. Indeed, the vibrational activity observed in the 1550 cm^{-1} region follows closely the IR absorption spectrum of P*. In addition, repopulation of the original state (I) is observed also (i.e. the quantum yield for isomerization is less than unity),[60] and the SAS of the second species contains contributions from both vibrationally hot ground-state I and metastable P* isomers. Vibrational cooling of these isomers leads to the SAS of the final species, which is in excellent agreement with the steady-state FTIR difference spectrum of room-temperature I and P*.

The present experimental and theoretical data allow a complete picture of the mechanism by which the molecular rotary motor undergoes isomerization after electronic excitation (Figure 3). Photon absorption brings the motor to a "bright" state from which it decays on an ultrafast time scale and within the time resolution of the present experiments to a different electronically excited "dark" state. In line with previous calculations on similar systems, our calculations indicate that this is a barrierless process proceeding via a conical intersection.[34] Previously, it was assumed that structural evolution on the HOMO → LUMO potential energy surface is responsible for the observed ultrafast decay of the fluorescence, and (following commonly accepted models on photoisomerization of carbon−carbon double bonds) that it primarily proceeds along torsional and pyramidalization coordinates.[74−76] The present study, in contrast, leads to the conclusion that the fluorescence decay is mediated by the passage through the conical intersection of the HOMO → LUMO and HOMO−1 → LUMO potential energy surfaces. Inspection of the structural changes that occur upon geometry relaxation to the minimum on the HOMO−1 → LUMO potential energy surface show that the central C=C bond length increases from 1.381 to 1.461 Å and that only relatively small changes occur in the torsional and pyramidalization coordinates. In combination with the forces that act on the molecule at the Franck−Condon excited "bright" state (Supplementary Figure 3), this suggests that motion along the C=C stretch coordinate needs to be taken into account as well for understanding the decay of the fluorescence.

Hence, it can be concluded that internal conversion to the electronic ground state takes place from the "dark" state. The decay rate for this process indicates that it is mediated by conical intersections between the two states as has indeed been proposed in previous theoretical studies.[34] These studies concluded, however, as well that to reach these intersections

DOI: 10.1021/acs.jpca.6b09644
J. Phys. Chem. A 2016, 120, 8606−8612

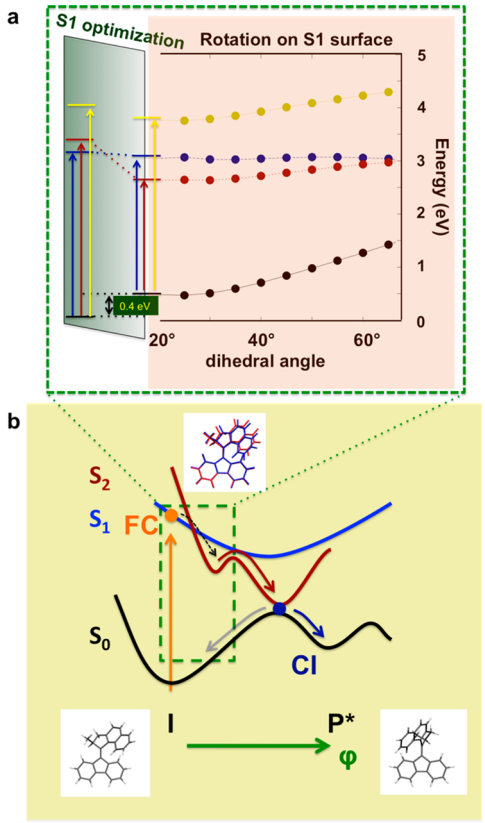

Figure 3. Proposed multistate dynamics of the photoinduced unidirectional rotation of the molecular motor starting from conformer I to conformer P* (projected into one dimension): dotted arrow, ultrafast process reported in previous work; fast (red arrow) and slow process (blue arrow) observed in the present time-resolved infrared study. (a) Calculated energy profile along the torsion coordinate showing how the energies of the electronic states change as the molecules evolves to conformer P*. (b) Schematic representation of the proposed model. Note that all stationary points were confirmed by normal-mode analysis.

a barrier needs to be overcome that results from the steric repulsion of the methyl group of the rotor unit with the hydrogen of the stator unit. Previous time-resolved fluorescence measurements reported an ultrafast damping mode at 113 cm^{-1} that was speculated to arise from motion along a coordinate involving inversion/pyramidalization although no direct support could be found for such an assignment.[42] Interestingly, our calculations find in the "dark" state a mode at 119 cm^{-1} (B3LYP/cc-pVDZ; not scaled, Supporting Information) that involves motion of the methyl group with respect to the hydrogen of the stator unit. One might therefore wonder to what extent this mode is related to the oscillatory behavior of the fluorescence. Our observed S_2 decay constant of 1.5 ps matches the slow component of the overall fluorescence decay (0.9−1.5 ps).[42] Our calculation of the excitation energies of the "bright" and "dark" states along the 119 cm^{-1} normal mode did not show a conical intersection between the two states, supporting the previous explanation of the oscillations observed in the fluorescence measurements[42] by the movement of wave packets and suggesting a scenario in which a coherent oscillation in the dark S_2 state periodically partly repopulates the fluorescent S_1 state. However, our experimental methods do not provide the time resolution to confirm this.

SUMMARY AND CONCLUSION

The photodynamics of a unidirectional molecular motor has been studied by time-resolved IR spectroscopy in which both vibrational and electronic structures are probed. In combination with quantum mechanical calculations, the high structural sensitivity and real-time character of the technique allows us to understand fundamental aspects of the operation mechanism. The results show that conversion of photon energy into directed motion proceeds on the potential energy surfaces of two different electronic states, which is the more important as it implies that the conical intersection between the "dark" electronically excited state and the ground state determines the efficiency of the motor. To rationally tune the performance of photoinitiated unidirectional rotation thus involves a multicoupled-state optimization of nuclear motion.

ASSOCIATED CONTENT

Supporting Information

The Supporting Information is available free of charge on the ACS Publications website at DOI: 10.1021/acs.jpca.6b09644.

Solvent response and power dependency of the transient IR signal, transient IR global data fitting and FTIR spectra, structure showing the gradient vectors acting on the molecule at the Frank−Condon point, structure of the dark state, structure showing the force vectors associated with the normal mode, vibrational band assignments of conformers I and P* (PDF)

Movie of the normal mode, I 1625.43 cm^{-1} (MOV); movie of the normal mode, I 1615.85 cm^{-1} (MOV); movie of the normal mode, I 1598.05 cm^{-1} (MOV); movie of the normal mode, I 1587.39 cm^{-1} (MOV); movie of the normal mode, I 1567.67 cm^{-1} (MOV); movie of the normal mode, P* 1611.44 cm^{-1} (MOV); movie of the normal mode, P* 1593.63 cm^{-1} (MOV); movie of the normal mode, P* 1576.22 cm^{-1} (MOV); movie of the normal mode, P* 1573.24 cm^{-1} (MOV); movie of the normal mode, P* 1557.31 cm^{-1} (MOV); movie of the normal mode, dark-state 119.44 cm^{-1} (MOV) (ZIP)

AUTHOR INFORMATION

Corresponding Authors

*S. Amirjalayer. E-mail: samir_01@uni-muenster.de. Telephone: +49 251 83 63919.

*W. J. Buma. E-mail: w.j.buma@uva.nl. Telephone: +31 20 525 6973.

*S. Woutersen. E-mail: s.woutersen@uva.nl. Telephone: +31 20 525 7091.

Notes

The authors declare no competing financial interest.

ACKNOWLEDGMENTS

S.A. thanks the Deutsche Akademie der Naturforscher Leopoldina−German National Academy of Sciences for a Leopoldina research fellowship (grant number LPDS 2011-18). S.W. acknowledges financial support from the John van Geuns foundation. B.L.F. acknowledges support from the European Research Council (Advanced Investigator Grant, No. 227897 to B.L.F.).

DOI: 10.1021/acs.jpca.6b09644
J. Phys. Chem. A 2016, 120, 8606−8612

REFERENCES

(1) Kay, E. R.; Leigh, D. A.; Zerbetto, F. Synthetic Molecular Motors and Mechanical Machines. *Angew. Chem., Int. Ed.* **2007**, *46*, 72−191.
(2) Coskun, A.; Banaszak, M.; Astumian, R. D.; Stoddart, J. F.; Grzybowski, B. A. Great Expectations: Can Artificial Molecular Machines Deliver on their Promise? *Chem. Soc. Rev.* **2012**, *41*, 19−30.
(3) Serreli, V.; Lee, C. F.; Kay, E. R.; Leigh, D. A. A Molecular Information Ratchet. *Nature* **2007**, *445*, 523−527.
(4) Browne, W. R.; Feringa, B. L. Making Molecular Machines Work. *Nat. Nanotechnol.* **2006**, *1*, 25−35.
(5) Sato, O.; Tao, J.; Zhang, Y.-Z. Control of Magnetic Properties through External Stimuli. *Angew. Chem., Int. Ed.* **2007**, *46*, 2152−2187.
(6) Galli, M.; Lewis, J. E. M.; Goldup, S. M. A Stimuli-Responsive Rotaxane−Gold Catalyst: Regulation of Activity and Diastereoselectivity. *Angew. Chem., Int. Ed.* **2015**, *54*, 13545−13549.
(7) Göstl, R.; Senf, A.; Hecht, S. Remote-Controlling Chemical Reactions by Light: Towards Chemistry with High Spatio-Temporal Resolution. *Chem. Soc. Rev.* **2014**, *43*, 1982−1996.
(8) Mura, S.; Nicolas, J.; Couvreur, P. Stimuli-Responsive Nanocarriers for Drug Delivery. *Nat. Mater.* **2013**, *12*, 991−1003.
(9) Fan, N.-C.; Cheng, F.-Y.; Ho, J.-A. A.; Yeh, C.-S. Photocontrolled Targeted Drug Delivery: Photocaged Biologically Active Folic Acid as a Light-Responsive Tumor-Targeting Molecule. *Angew. Chem., Int. Ed.* **2012**, *51*, 8806−8810.
(10) Fehrentz, T.; Schönberger, M.; Trauner, D. Optochemical Genetics. *Angew. Chem., Int. Ed.* **2011**, *50*, 12156−12182.
(11) Abendroth, J. M.; Bushuyev, O. S.; Weiss, P. S.; Barrett, C. J. Controlling Motion at the Nanoscale: Rise of the Molecular Machines. *ACS Nano* **2015**, *9*, 7746−7768.
(12) Bléger, D.; Hecht, S. Visible-Light-Activated Molecular Switches. *Angew. Chem., Int. Ed.* **2015**, *54*, 11338−11349.
(13) García-Amorós, J.; Velasco, D. Recent Advances towards Azobenzene-based Light-Driven Real-Time Information-transmitting Materials. *Beilstein J. Org. Chem.* **2012**, *8*, 1003−1017.
(14) Bandara, H. M. D.; Burdette, S. C. Photoisomerization in Different Classes of Azobenzene. *Chem. Soc. Rev.* **2012**, *41*, 1809−1825.
(15) Waldeck, D. H. Photoisomerization Dynamics of Stilbenes. *Chem. Rev.* **1991**, *91*, 415−436.
(16) Michl, J.; Sykes, E. C. H. Molecular Rotors and Motors: Recent Advances and Future Challenges. *ACS Nano* **2009**, *3*, 1042−1048.
(17) Pathem, B. K.; Claridge, S. A.; Zheng, Y. B.; Weiss, P. S. Molecular Switches and Motors on Surfaces. *Annu. Rev. Phys. Chem.* **2013**, *64*, 605−630.
(18) Russew, M.-M.; Hecht, S. Photoswitches: From Molecules to Materials. *Adv. Mater.* **2010**, *22*, 3348−3360.
(19) Morgenstern, K. Switching Individual Molecules by Light and Electrons: From Isomerisation to Chirality Flip. *Prog. Surf. Sci.* **2011**, *86*, 115−161.
(20) Köhntopp, A.; Dabrowski, A.; Malicki, M.; Temps, F. Photoisomerisation and Ligand-controlled Reversible Aggregation of Azobenzene-Functionalised Gold Nanoparticles. *Chem. Commun.* **2014**, *50*, 10105−10107.
(21) Siewertsen, R.; Neumann, H.; Buchheim-Stehn, B.; Herges, R.; Näther, C.; Renth, F.; Temps, F. Highly Efficient Reversible Z−E Photoisomerization of a Bridged Azobenzene with Visible Light through Resolved S1($n\pi^*$) Absorption Bands. *J. Am. Chem. Soc.* **2009**, *131*, 15594−15595.
(22) Steinwand, S.; Halbritter, T.; Rastädter, D.; Ortiz-Sánchez, J. M.; Burghardt, I.; Heckel, A.; Wachtveitl. Ultrafast Spectroscopy of Hydroxy-Substituted Azobenzenes in Water. J. *Chem. - Eur. J.* **2015**, *21*, 15720−15731.
(23) Wachtveitl, J.; Zumbusch, A. Azobenzene: An Optical Switch for in vivo Experiments. *ChemBioChem* **2011**, *12*, 1169−1170.
(24) Greb, L.; Lehn, J.-M. Light-Driven Molecular Motors: Imines as Four-Step or Two-Step Unidirectional Rotors. *J. Am. Chem. Soc.* **2014**, *136*, 13114−13117.
(25) Greb, L.; Eichhöfer, A.; Lehn, J.-M. Synthetic Molecular Motors: Thermal N Inversion and Directional Photoinduced C═N Bond Rotation of Camphorquinone Imines. *Angew. Chem., Int. Ed.* **2015**, *54*, 14345−14348.
(26) Haberhauer, G.; Burkhart, C.; Woitschetzki, S.; Wölper, C. Light and Chemically Driven Molecular Machines Showing a Unidirectional Four-State Switching Cycle. *J. Org. Chem.* **2015**, *80*, 1887−1895.
(27) Guentner, M.; Schildhauer, M.; Thumser, S.; Mayer, P.; Stephenson, D.; Mayer, P. J.; Dube, H. Sunlight-powered kHz Rotation of a Hemithioindigo-based Molecular Motor. *Nat. Commun.* **2015**, *6*, 8406.
(28) Bléger, D.; Ciesielski, A.; Samorì, P.; Hecht, S. Photoswitching Vertically Oriented Azobenzene Self-Assembled Monolayers at the Solid−Liquid Interface. *Chem. - Eur. J.* **2010**, *16*, 14256−14260.
(29) Ube, T.; Ikeda, T. Photomobile Polymer Materials with Crosslinked Liquid-Crystalline Structures: Molecular Design, Fabrication, and Functions. *Angew. Chem., Int. Ed.* **2014**, *53*, 10290−10299.
(30) Wang, Y.; Li, Q. Light-Driven Chiral Molecular Switches or Motors in Liquid Crystals. *Adv. Mater.* **2012**, *24*, 1926−1945.
(31) Coti, K. K.; Belowich, M. E.; Liong, M.; Ambrogio, M. W.; Lau, Y. A.; Khatib, H. A.; Zink, J. I.; Khashab, N. M.; Stoddart, J. F. Mechanised Nanoparticles for Drug Delivery. *Nanoscale* **2009**, *1*, 16−39.
(32) Fujiwara, M.; Akiyama, M.; Hata, M.; Shiokawa, K.; Nomura, R. Photoinduced Acceleration of the Effluent Rate of Developing Solvents in Azobenzene-Tethered Silica Gel. *ACS Nano* **2008**, *2*, 1671−1681.
(33) Koumura, N.; Zijlstra, R. W. J.; van Delden, R. A.; Harada, N.; Feringa, B. L. Light-driven Monodirectional Molecular Rotor. *Nature* **1999**, *401*, 152−155.
(34) Liu, F.; Morokuma, K. Computational Study on the Working Mechanism of a Stilbene Light-Driven Molecular Rotary Motor: Sloped Minimal Energy Path and Unidirectional Nonadiabatic Photoisomerization. *J. Am. Chem. Soc.* **2012**, *134*, 4864−4876.
(35) Kazaryan, A.; Filatov, M. Density Functional Study of the Ground and Excited State Potential Energy Surfaces of a Light-Driven Rotary Molecular Motor (3R,3′R)-(P,P)-trans-1,1′,2,2′,3,3′,4,4′-Octahydro-3,3′-dimethyl-4,4′-biphenanthrylidene. *J. Phys. Chem. A* **2009**, *113*, 11630−11634.
(36) Amatatsu, Y. Theoretical Design of a Light-Driven Molecular Rotary Motor with Low Energy Helical Inversion: 9-(5-Methyl-2-phenyl-2-cyclopenten-1-ylidene)-9H-fluorene. *J. Phys. Chem. A* **2013**, *117*, 12529−12539.
(37) Kazaryan, A.; Kistemaker, J. C. M.; Schäfer, L. V.; Browne, W. R.; Feringa, B. L.; Filatov, M. Understanding the Dynamics Behind the Photoisomerization of a Light-Driven Fluorene Molecular Rotary Motor. *J. Phys. Chem. A* **2010**, *114*, 5058−5067.
(38) Filatov, M. Understanding the Dynamics behind Photoisomerization of Light-driven Molecular Rotary Motors. *WIREs Comput. Mol. Sci.* **2013**, *3*, 427−437.
(39) Kazaryan, A.; Lan, Z.; Schäfer, L. V.; Thiel, W.; Filatov, M. Surface Hopping Excited-State Dynamics Study of the Photoisomerization of a Light-Driven Fluorene Molecular Rotary Motor. *J. Chem. Theory Comput.* **2011**, *7*, 2189−2199.
(40) Fang, C.; Oruganti, B.; Durbeej, B. Computational Study of the Working Mechanism and Rate Acceleration of Overcrowded Alkene-based Light-driven Rotary Molecular Motors. *RSC Adv.* **2014**, *4*, 10240−10251.
(41) Filatov, M.; Olivucci, M. Designing Conical Intersections for Light-Driven Single Molecule Rotary Motors: From Precessional to Axial Motion. *J. Org. Chem.* **2014**, *79*, 3587−3600.
(42) Augulis, R.; Klok, M.; Feringa, B. L.; van Loosdrecht, P. H. M. Light-driven Rotary Molecular Motors: an Ultrafast Optical Study. *Phys. Status Solidi C* **2009**, *6*, 181−184.
(43) Conyard, J.; Cnossen, A.; Browne, W. R.; Feringa, B. L.; Meech, S. R. Chemically Optimizing Operational Efficiency of Molecular Rotary Motors. *J. Am. Chem. Soc.* **2014**, *136*, 9692−9700.
(44) Conyard, J.; Addison, K.; Heisler, I. A.; Cnossen, A.; Browne, W. R.; Feringa, B. L.; Meech, S. R. Ultrafast Dynamics in the Power Stroke of a Molecular Rotary Motor. *Nat. Chem.* **2012**, *4*, 547−551.

DOI: 10.1021/acs.jpca.6b09644
J. Phys. Chem. A 2016, 120, 8606−8612

(45) McMahon, S.; Amirjalayer, S.; Buma, W. J.; Halpin, Y.; Long, C.; Rooney, A. D.; Woutersen, S.; Pryce, M. T. An Investigation into the Photochemistry of, and the Electrochemically induced CO-loss from, $[(CO)_5MC(OMe)Me]$(M = Cr or W) using Low-temperature Matrix Isolation, Picosecond Infrared Spectroscopy, Cyclic Voltammetry, and Time-Dependent Density Functional Theory. *Dalton Trans.* **2015**, *44*, 15424−15343.
(46) *Turbomole* V6.1, a Development of the University of Karlsruhe and Forschungszentrum Karlsruhe GmbH, 1989−2007, TURBOMOLE GmbH since 2007, http://www.turbomole.com.
(47) Stephens, P. J.; Devlin, F. J.; Chabalowski, C. F.; Frisch, M. J. Ab Initio Calculation of Vibrational Absorption and Circular Dichroism Spectra Using Density Functional Force Fields. *J. Phys. Chem.* **1994**, *98*, 11623−11627.
(48) Grimme, S.; Antony, J.; Ehrlich, S.; Krieg, H. A Consistent and Accurate Ab Initio Parametrization of Density Functional Dispersion Correction (DFT-D) for the 94 Elements H-Pu. *J. Chem. Phys.* **2010**, *132*, 154104.
(49) Wilson, A. K.; Woon, D. E.; Peterson, K. A.; Dunning, T. H. Gaussian Basis Sets for use in Correlated Molecular Calculations. IX. The Atoms Gallium through Krypton. *J. Chem. Phys.* **1999**, *110*, 7667−7676.
(50) Weigend, F.; Köhn, A.; Hättig, C. Efficient use of the Correlation Consistent Basis Sets in Resolution of the Identity MP2 Calculations. *J. Chem. Phys.* **2002**, *116*, 3175−3183.
(51) Grimme, S. Improved second-order Møller−Plesset perturbation theory by separate scaling of parallel- and antiparallel-spin pair correlation energies. *J. Chem. Phys.* **2003**, *118*, 9095−9102.
(52) Eichkorn, K.; Weigend, F.; Treutler, O. Auxiliary Basis Sets for Main Row Atoms and Transition Metals and their use to Approximate Coulomb Potentials. *Theor. Chem. Acc.* **1997**, *97*, 119−124.
(53) Hättig, C.; Weigend, F. CC2 Excitation Energy Calculations on Large Molecules using the Resolution of the Identity Approximation. *J. Chem. Phys.* **2000**, *113*, 5154−5161.
(54) Frisch, M. J.; Trucks, G. W.; Schlegel, H. B.; Scuseria, G. E.; Robb, M. A.; Cheeseman, J. R.; Scalmani, G.; Barone, V.; Mennucci, B.; Petersson, G. A.; et al. *Gaussian 09*, revision D.01; Gaussian, Inc.: Wallingford, CT, 2009.
(55) Becke, A. D. Density-Functional Exchange-Energy Approximation with Correct Asymptotic Behavior. *Phys. Rev. A: At., Mol., Opt. Phys.* **1988**, *38*, 3098−3100.
(56) Lee, C.; Yang, W.; Parr, R. G. Development of the Colle-Salvetti Correlation-Energy Formula into a Functional of the Electron Density. *Phys. Rev. B: Condens. Matter Mater. Phys.* **1988**, *37*, 785−789.
(57) Stephens, P. J.; Devlin, F. J.; Chabalowski, C. F.; Frisch, M. J. Ab Initio Calculation of Vibrational Absorption and Circular Dichroism Spectra Using Density Functional Force Fields. *J. Phys. Chem.* **1994**, *98*, 11623−11627.
(58) Figgen, D.; Rauhut, G.; Dolg, M.; Stoll, H. Energy-Consistent Pseudopotentials for Group 11 and 12 Atoms: Adjustment to Multi-Configuration Dirac−Hartree−Fock Data. *Chem. Phys.* **2005**, *311*, 227−244.
(59) Peterson, K. A.; Puzzarini, C. Systematically Convergent Basis Sets for Transition Metals. II. Pseudopotential-based Correlation Consistent Basis Sets for the Group 11 (Cu, Ag, Au) and 12 (Zn, Cd, Hg) Elements. *Theor. Chem. Acc.* **2005**, *114*, 283−296.
(60) Vicario, J.; Meetsma, A.; Feringa, B. L. Controlling the Speed of Rotation in Molecular Motors. Dramatic Acceleration of the Rotary Motion by Structural Modification. *Chem. Commun.* **2005**, 5910−5912.
(61) Hamm, P.; Ohline, S. M.; Zinth, W. Vibrational Cooling after Ultrafast Photoisomerization of Azobenzene Measured by Femtosecond Infrared Spectroscopy. *J. Chem. Phys.* **1997**, *106*, 519−529.
(62) Neumann-Verhoefen, M.-K.; Neumann, K.; Bamann, C.; Radu, I.; Heberle, J.; Bamberg, E.; Wachtveitl, J. Ultrafast Infrared Spectroscopy on Channelrhodopsin-2 Reveals Efficient Energy Transfer from the Retinal Chromophore to the Protein. *J. Am. Chem. Soc.* **2013**, *135*, 6968−6976.
(63) Neumann, K.; Verhoefen, M.-K.; Mewes, J.-M.; Dreuw, A.; Wachtveitl, J. Investigating the CO2 Uncaging Mechanism of Nitrophenylacetates by Means of fs-IR Spectroscopy and Quantum Chemical Calculations. *Phys. Chem. Chem. Phys.* **2011**, *13*, 17367−17377.
(64) Laimgruber, S.; Schreier, W. J.; Schrader, T.; Koller, F.; Zinth, W.; Gilch, P. The Photochemistry of o-Nitrobenzaldehyde as Seen by Femtosecond Vibrational Spectroscopy. *Angew. Chem., Int. Ed.* **2005**, *44*, 7901−7904.
(65) Heyne, K.; Mohammed, O. F.; Usman, A.; Dreyer, J.; Nibbering, E. T. J.; Cusanovich, M. A. Structural Evolution of the Chromophore in the Primary Stages of Trans/Cis Isomerization in Photoactive Yellow Protein. *J. Am. Chem. Soc.* **2005**, *127*, 18100−18106.
(66) Torres-Alacan, J.; Das, U.; Filippou, A. C.; Vöhringer, P. Observing the Formation and the Reactivity of an Octahedral Iron(V) Nitrido Complex in Real Time. *Angew. Chem., Int. Ed.* **2013**, *52*, 12833−12837.
(67) Li, P.; Amirjalayer, S.; Hartl, F.; Lutz, M.; de Bruin, B.; Becker, R.; Woutersen, S.; Reek, J. N. H. Direct Probing of Photoinduced Electron Transfer in a Self-Assembled Biomimetic [2Fe2S]-Hydrogenase Complex Using Ultrafast Vibrational Spectroscopy. *Inorg. Chem.* **2014**, *53*, 5373−5383.
(68) Salem, L. Theory of Photochemical Reactions. *Science* **1976**, *191*, 822−830.
(69) Wiberg, K. B.; Hadad, C. M.; Foresman, J. B.; Chupka, W. A. Electronically Excited States of Ethylene. *J. Phys. Chem.* **1992**, *96*, 10756−10768.
(70) Krawczyk, R. P.; Viel, A.; Manthe, U.; Domcke, W. Photoinduced Dynamics of the Valence States of Ethene: A Six-dimensional Potential-Energy Surface of Three Electronic States with several Conical Intersections. *J. Chem. Phys.* **2003**, *119*, 1397−1411.
(71) Zijlstra, R. W. J.; van Duijnen, P. T.; Feringa, B. L.; Steffen, T.; Duppen, K.; Wiersma, D. A. Excited-State Dynamics of Tetraphenylethylene: Ultrafast Stokes Shift, Isomerization, and Charge Separation. *J. Phys. Chem. A* **1997**, *101*, 9828−9836.
(72) Han, W.-G.; Lovell, T.; Liu, T.; Noodleman, L. Density Functional Studies of the Ground- and Excited-State Potential-Energy Curves of Stilbene cis−trans Isomerization. *ChemPhysChem* **2002**, *3*, 167−178.
(73) Levine, B. G.; Martinez, T. J. Ab Initio Multiple Spawning Dynamics of Excited Butadiene: Role of Charge Transfer. *J. Phys. Chem. A* **2009**, *113*, 12815−12824.
(74) Nenov, A.; Cordes, T.; Herzog, T. T.; Zinth, W.; de Vivie-Riedle, R. Molecular Driving Forces for Z/E Isomerization Mediated by Heteroatoms: The Example Hemithioindigo. *J. Phys. Chem. A* **2010**, *114*, 13016−13030.
(75) Marchand, G.; Eng, J.; Schapiro, I.; Valentini, A.; Frutos, L. M.; Pieri, E.; Olivucci, M.; Léonard, J.; Gindensperger, E. Directionality of Double-Bond Photoisomerization Dynamics Induced by a Single Stereogenic Center. *J. Phys. Chem. Lett.* **2015**, *6*, 599−604.
(76) Maerz, B.; Wiedbrauk, S.; Oesterling, S.; Samoylova, E.; Nenov, A.; Mayer, P.; de Vivie-Riedle, R.; Zinth, W.; Dube, H. Making Fast Photoswitches Faster—Using Hammett Analysis to Understand the Limit of Donor−Acceptor Approaches for Faster Hemithioindigo Photoswitches. *Chem. - Eur. J.* **2014**, *20*, 13984−13992.

DOI: 10.1021/acs.jpca.6b09644
J. Phys. Chem. A 2016, 120, 8606−8612